Radiation Measurements 177 (2024) 107262

Contents lists available at ScienceDirect

Radiation Measurements

journal homepage: www.elsevier.com/locate/radmeas

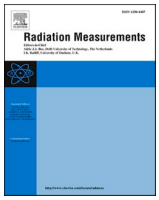

Investigating thermoluminescence signal saturation in quartz and feldspar using emission spectrometry

Pontien Niyonzima *, Salome Oehler, Georgina E. King, Christoph Schmidt

Institute of Earth Surface Dynamics, University of Lausanne, Géopolis, 1015, Lausanne, Switzerland

A B S T R A C T

Luminescence-based thermometry and dating often requires determination of the saturation level for specific signals and the corresponding dose. However, previous studies found non-monotonic dose responses for some monochromatic thermoluminescence (TL) and optically stimulated luminescence (OSL) signals from quartz as well as spectral overlap of emission bands, substantially complicating data interpretation. Therefore, the present study examines (1) the variability in the TL emission spectrum of quartz and feldspar from bedrock and sediment of different provenances and, (2) the saturation characteristics of the blue emission band for both quartz and feldspar in the dose range from 0.25 kGy to 50 kGy. The experimental results confirm differences in the spectra which appear to be characteristic of their geological origin and chemical composition. Spectral analysis shows that in the temperature range 175–220 °C the blue emission band at ~2.5 eV dominates over other bands for all quartz samples studied. A broad UV-blue TL signal peaking at ~2.5–3.0 eV and composed of probably three overlapping, individual bands is characteristic for K-feldspar, while one Na-feldspar exhibits an additional band at ~2.2 eV.

In the studied dose range, the emissions at ~2.5 eV and ~2.6 eV increase as a function of dose up to 6 kGy for both quartz and feldspar. A difference in dose response was observed for high doses (>6 kGy) where feldspar samples reached a stable saturation level while for quartz the blue emission band intensity decays until 50 kGy after having attained a maximum. Our results suggest the suitability of feldspar TL for palaeothermometry and thermochronometry from the perspective of signal saturation characteristics. However, the spectral overlap of several bands in the UV-blue emission requires careful optical filter selection to isolate the signal of interest. The non-monotonic dose response of the ~2.5 eV emission of quartz around 200 °C glow curve temperature probably precludes its use for temperature sensing based on relative trap saturation levels.

1. Introduction

The luminescence characteristics of quartz and feldspar have been extensively studied and used for Quaternary geochronology and thermochronology research in the past decades (e.g., Fattahi and Stokes, 2000, 2003; King et al., 2016a; Preusser et al., 2009; Zhang and Li, 2020; Murari et al., 2021). In particular, feldspar has received increased attention since the development of routines correcting for anomalous fading (e.g., Wintle, 1973; Huntley and Lamothe, 2001) and of protocols reducing this unwanted effect (e.g., Thomsen et al., 2008). Beyond pure chronometric applications, quartz and feldspar luminescence is being increasingly exploited to study Earth surface processes (e.g., Gray et al., 2019) and the interactions between climate, tectonics and erosion to constrain the rate and timing of landscape evolution (e.g., Herman et al., 2010; Tang and Li, 2015; King et al., 2016a,b; Brown et al., 2017; Herman and King, 2018; King et al., 2020; Stalder et al., 2022).

Recently, thermoluminescence (TL) of feldspar was proposed as a palaeothermometer to constrain temporal variations of Earth's surface air temperature within the last few tens of thousands of years (Biswas et al., 2020). Early work on using TL of natural minerals to reconstruct rock thermal histories goes back to Ronca and Zeller (1965), Christodoulides et al. (1971), Durrani et al. (1972, 1977) and Guimon et al. (1984). TL palaeothermometry is based on the temperature-dependent electron trapping and detrapping in feldspar or quartz minerals. The method uses metastable signals appearing at ~180–250 °C in the TL glow curve, which are sensitive to temperature fluctuations occurring at Earth's surface over geological timescales. To infer the temperature history of a rock sample, the relative trap saturation of specific signals is determined along with their kinetic parameters (Biswas et al., 2020). These kinetic parameters, that describe the luminescence signal's evolution as a function of irradiation and thermal treatments, are estimated for each sample through a series of laboratory experiments. Since laboratory results are thus extrapolated to geological time scales, slight inaccuracies may have large effects on the temperature reconstruction. Therefore, further investigations are required to constrain the physical parameters describing TL growth and decay in response to irradiation

* Corresponding author.
E-mail address: pontien.niyonzima@unil.ch (P. Niyonzima).

https://doi.org/10.1016/j.radmeas.2024.107262
Received 2 April 2024; Received in revised form 25 July 2024; Accepted 29 July 2024
Available online 31 July 2024

and ambient temperature fluctuations as accurately as possible, which is central not only for palaeothermometry and thermochronometry, but also for improving the accuracy of luminescence dating.

Determining the relative trap saturation (normally given as a fraction of 1, with a value of 0.5 indicating that 50% of the available traps are filled) involves measuring the natural signal and comparing it to the signal in dose saturation. The latter needs to be measured in the laboratory by administering doses high enough to cease further signal growth.

In the case of feldspar, a correction is required to account for anomalous fading to obtain the luminescence signal corresponding to field saturation (cf. Kars et al., 2008). However, previous studies highlighted potential complications in identifying an unambiguous dose saturation level.

1. For TL and optically stimulated luminescence (OSL) of some quartz samples, signal growth at high laboratory doses (>500–1000 Gy) has been reported that is not compatible with exponential saturation (Woda et al., 2002). Dose response data in such cases can be best fitted with either an exponential plus linear or a double-exponential function (Lowick et al., 2010; Rahimzadeh et al., 2021) or show non-monotonic behaviour (i.e., decreasing intensity with dose; Anechitei-Deacu et al., 2018; Autzen et al., 2021). These observations imply that at least in the dose range studied a saturation level cannot be quantified unequivocally.
2. Unexpected dose response behaviour at high doses using monochromatic quartz TL signals (measured using optical filters in front of a photomultiplier tube) could be traced back to changes in the relative proportion of individual TL emissions as a function of dose and/or following heat treatments (Bøtter-Jensen et al., 1995; Schilles et al., 2001; Woda et al., 2002; Hunter et al., 2018; Schmidt and Woda, 2019). Using conventional TL measurements and without additional spectrometric information, interfering TL emissions with differing dose response characteristics could impede determination of an accurate saturation level of the signal/emission of interest (Kuhn et al., 2000).

In this study, we address this problem by investigating the effects of laboratory irradiation and heating on TL emission spectra of quartz and feldspar from bedrock and sediment of different provenances. Three-dimensional TL spectra capture a maximum of information and allow defects in crystals relevant for luminescence dating and thermometry to be studied in detail (Scholefield and Prescott, 1999): the position of emission peaks on the temperature axis characterises the physical properties of traps from which electrons are released upon heating, whilst the spectral emission bands provide information about recombination centres. We expect this new data to provide crucial information as to which metastable quartz and feldspar TL emissions yield well-defined dose saturation intensities allowing the accuracy of past temperature histories determined using luminescence-based palaeothermometry to be further improved.

2. Materials and methods

We investigated four feldspar samples from bedrock and three quartz samples from sediment; their provenance is given in Table 1. Both

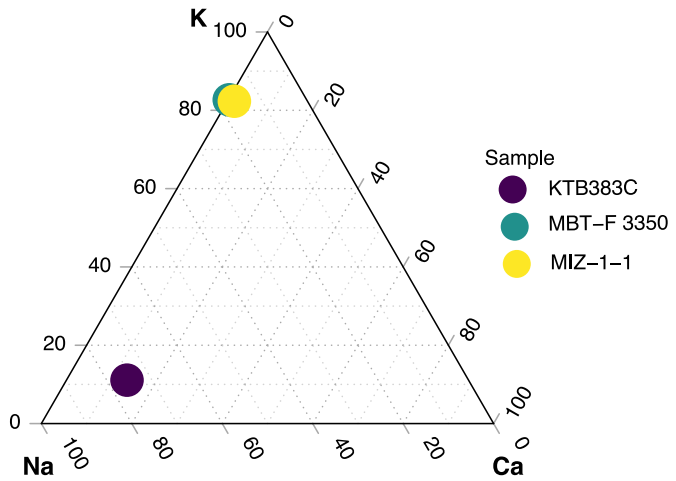

Fig. 1. Ternary plot of feldspar geochemistry based on XRF. The investigated samples are marked with circles and each colour corresponds to different samples as shown in the legend.

bedrock and sediment samples were prepared following standard routines (e.g., Preusser et al., 2008; King et al., 2016c) to give coarse grains (fine sand) for analysis. In this study, we examined both K-feldspar and Na-feldspar to investigate potential changes in the structure of TL spectra with geochemical composition. We performed X-ray fluorescence (XRF) analysis to characterise the feldspar separates studied here (Fig. 1).

TL spectral measurements were carried out at the University of Lausanne using an Andor Kymera 193i spectrograph for wavelength-dispersion in combination with a UV-enhanced Andor iXon Ultra 888 electron multiplying charge-coupled device (EMCCD, 300–900 nm) camera attached to the Detection and Stimulation Head (DASH) system of an automated Risø TL/OSL-DA-20 reader. The EMCCD has a 1024 x 1024-pixel sensor format and a pixel size of 13 μm. A system of fused silica lenses focusses the light emitted by the sample onto the end of a fiber bundle (diameter: 3.1 mm, numerical aperture: 0.22) that transmits the light onto the entrance slit of the spectrograph. The spectral resolution of the system is 13 nm for all spectra presented here. We set the horizontal shift readout to 30 MHz, vertical shift speed to 4.33 μs, and the grating of the spectrograph to 150 lines mm^{-1} and 500 nm blaze. The TL spectra were taken without band filters to capture the full spectrum between 281 and 717 nm, energy and efficiency calibrated and cleared from spikes induced by cosmic rays. The efficiency calibration was carried out by comparing the known emission spectrum in free space (in terms of irradiance) of a Bentham CL2 100 W quartz halogen calibration lamp with the spectrum of this lamp as recorded by the spectrometric system. Samples that produced bright TL signals were used in the investigation of the dose response characteristics of quartz and feldspar.

Multi-grain aliquots (6 mm) were mounted on stainless steel discs and recorded without any optical filters for quartz samples, while a neutral density filter (optical density of 0.2, transmission of ~60%) was used for feldspar samples to avoid saturation of the EMCCD. Absolute

Table 1
Samples used in this study.

Lab code	Minerals	Grain size (μm)	Type	Provenance	Country
MBT-F 3350	K-feldspar	180–212	Bedrock	Mont Blanc	France (Lambert, 2018)
MIZ-1-1		180–250		Tono region	Japan (Ogata et al., 2022)
MIZ-1-8		180–250			
KTB383C	Na-feldspar	180–250		Windischeschenbach	Germany (Guralnik et al., 2015)
BT1799	Quartz	80–200	Sediment	Foum	Cameroon
BT1651		90–125		Matmata	Tunisia
BP5.5		180–212		Chobe Enclave	Botswana (Vainer et al.)

Table 2
Protocol used in this study to characterise samples for their spectrally resolved TL dose response.

Steps	Treatment
1	Natural TL spectrum up to 250 °C at 1 °C s^{-1}
2	Regenerative dose (up to 50 kGy)
3	TL spectrum up to 250 °C at 1 °C s^{-1} (signal)
4	Test dose (500 Gy)
5	TL spectrum up to 250 °C at 1 °C s^{-1} (test dose signal)
6	TL up to 450 °C (erase all remnant signal)
7	TL spectrum up to 250 °C at 1 °C s^{-1} (background)
8	Repeat steps 2 to 7

intensities for quartz and feldspar spectra are therefore not directly comparable.

We used two different approaches in this study: (1) screening samples by measuring spectra up to 350 °C for doses from 250 Gy to 1 kGy, (2) recording the dose response of spectra up to 250 °C for a much larger dose range (up to 50 kGy).

For the first approach, the aliquots were given regenerative doses ranging from 250 Gy to 1 kGy by means of a $^{90}Sr/^{90}Y$ beta-source (~0.16 Gy s^{-1}), and TL measurements were made by heating the samples to 350 °C at a rate of 1 °C s^{-1}, detecting the emitted light as a function of wavelength and temperature. After measurement of the TL spectra, we heated the sample up to 450 °C using the same aliquot to erase all remnant signals before recording the spectrally resolved instrumental background up to 350 °C which was subtracted from the initial TL spectrum. Based on the results of this experiment, bright samples (Table 1) and the temperature range of interest for further analysis could be appropriately selected.

For saturation dose investigations, a single aliquot regenerative dose (SAR) protocol (Table 2) was used. To minimise the influence of black body radiation at temperatures >300 °C, we measured TL spectra up to 250°C, that encompassed the TL signals of main interest for thermochronometry and palaeothermometry (Biswas et al., 2018, 2020). A test dose signal was also measured to correct for sensitivity change due to sample treatments.

Background-corrected TL spectra were visualised with the function plot_RLum.Data.Spectrum() as part of the R package 'Luminescence' (v0.9.23; Kreutzer et al., 2012; Kreutzer, 2023a). Transformation of TL spectra from wavelength to energy space and their decomposition into a variable number of Gaussian components was achieved using the function fit_EmissionSpectra() (Kreutzer, 2023b) of the R package referenced above, employing the Marquardt-Levenberg minimisation routine.

3. Results and discussion

3.1. Thermoluminescence emission spectra of quartz

The characteristics (number, position, and intensity) of TL emission bands from quartz were examined with TL spectrometry from room temperature to 350 °C after a laboratory dose up to 1 kGy. The studied samples produced only a very weak natural TL signal which might be due to the low natural dose (data not shown).

We first describe 3D and 2D spectra of the studied samples, as a basis for characterisation and screening of samples for decomposition and dose response behaviour analysis. For quartz, a blue emission with variable intensity was detected in all samples (Fig. 2). The spectra shown in Fig. 2 are evidently composite, the main emission being around 480 nm. Spectra of quartz samples irradiated with doses up to 1 kGy are characterised by at least four TL peaks at ~80 °C, ~150 °C, ~200 °C and ~320 °C when TL is measured at 1 °C s^{-1} heating rate (which correspond to the "110 °C", "160 °C", "210 °C" and "325 °C" TL peaks described in the literature; Krbetschek et al., 1997; Preusser et al., 2009). After beta-irradiation, the TL signal of sample BT1799 is dominated by the 200 °C peak (Fig. 2a and d), while the low temperature (80 °C and 150 °C) and high temperature peaks (320 °C) are still apparent. The common feature for all TL peaks of this sample is that they occur exclusively in the blue emission band (around 480 nm). Interestingly, the so-called 110 °C TL peak usually linked to an intense ultraviolet (UV) emission in quartz (e.g., Preusser et al., 2009) is completely absent in this sample.

This blue emission band is present also in the spectra of the other two quartz samples (BP5.5 and BT1651) but accompanied by supplementary emission bands. A UV emission around 380 nm and a red emission around 630 nm can be noted for sample BP5.5. For both the 80 °C and 200 °C TL peaks, blue and UV emissions are clearly present, and there is an indication of a red emission at ~200 °C, but it is not well defined.

Sample BT1651 exhibits a low-temperature (<100 °C) UV emission along with the signals described for the other two quartz samples (Fig. 2). For regenerative doses <4 kGy, the TL spectra of sample BT1651 are composed of UV, blue and red emissions which show peaks at temperatures of ~80 °C, ~200 °C and >350 °C. For the 200 °C TL peak, red (visible clearly after spectra decomposition) and blue emissions were observed. The 480 nm (2.5 eV) band dominates all other TL emissions for doses exceeding 1 kGy. As this emission is by far the most intense one in the studied samples and in the temperature range of interest for palaeothermometry, its dose response was investigated in detail in Section 3.4. We report the presence of at least three emission bands located at 1.9 eV, 2.5 eV and 3.2 eV in our samples, consistent with previous TL spectral studies of a range of quartz samples (e.g., Hashimoto et al., 1986; Rink et al., 1993; Kuhn et al., 2000). The spectral composition of the TL emission is associated with quartz origin and formation conditions (Preusser et al., 2009), but examining this in more detail is beyond the scope of this study.

3.2. Thermoluminescence emission spectra of feldspar

Fig. 3 shows TL spectra of feldspar samples from different provenances and of various geochemical compositions (MIZ-1-1 and MBT-F 3350: K-feldspar; KTB383C: Na-feldspar; see Fig. 1) after artificial beta-irradiation. The spectra (2D and 3D) of MIZ-1-8 (not presented here) are similar to that of MIZ-1-1, probably due to the same provenance and chemical composition.

All samples show a dominant emission at ~430 nm, while for the Na-feldspar sample (KTB383C) another emission band centred at ~580 nm with almost the same intensity is apparent. An emission band with its maximum intensity beyond 700 nm is apparent but our instrument was not able to record the full emission band due to its wavelength range limit (717 nm). It probably represents the far-red emission at ~710 nm described by Visocekas and Guérin (2006), reported to be free from anomalous fading. The common feature for TL spectra of irradiated feldspar samples is that in temperature space, the signal forms a broad continuum between ~70 °C and 250 °C. This observation is consistent with earlier studies, demonstrating that the K-feldspar TL glow curve is composed of numerous, closely spaced sub-peaks with a (quasi-) continuous distribution of activation energies (Kirsh et al., 1987). The position on the temperature axis of the TL maximum intensity is identical for the ~430 nm emission and the >700 nm emission for sample MIZ-1-8, suggesting that the same population of trapped electrons recombines at different luminescent centres. In contrast to the K-feldspar samples, the ~430 nm emission exhibits a second peak (or at least a pronounced shoulder) at ~250 °C for the Na-feldspar sample (Fig. 3c and f). The ~580 nm emission of this sample shows a similar pattern, although less distinct. It appears that the maximum TL intensity of the ~580 nm emission is reached at slightly higher glow curve temperatures (~140–150 °C), as compared to the ~430 nm emission, where the maximum occurs at ~110–130 °C. In wavelength space, emissions from feldspar appear to be broader and less discrete than those from quartz, which might be an effect of the overall differences in TL signal intensities

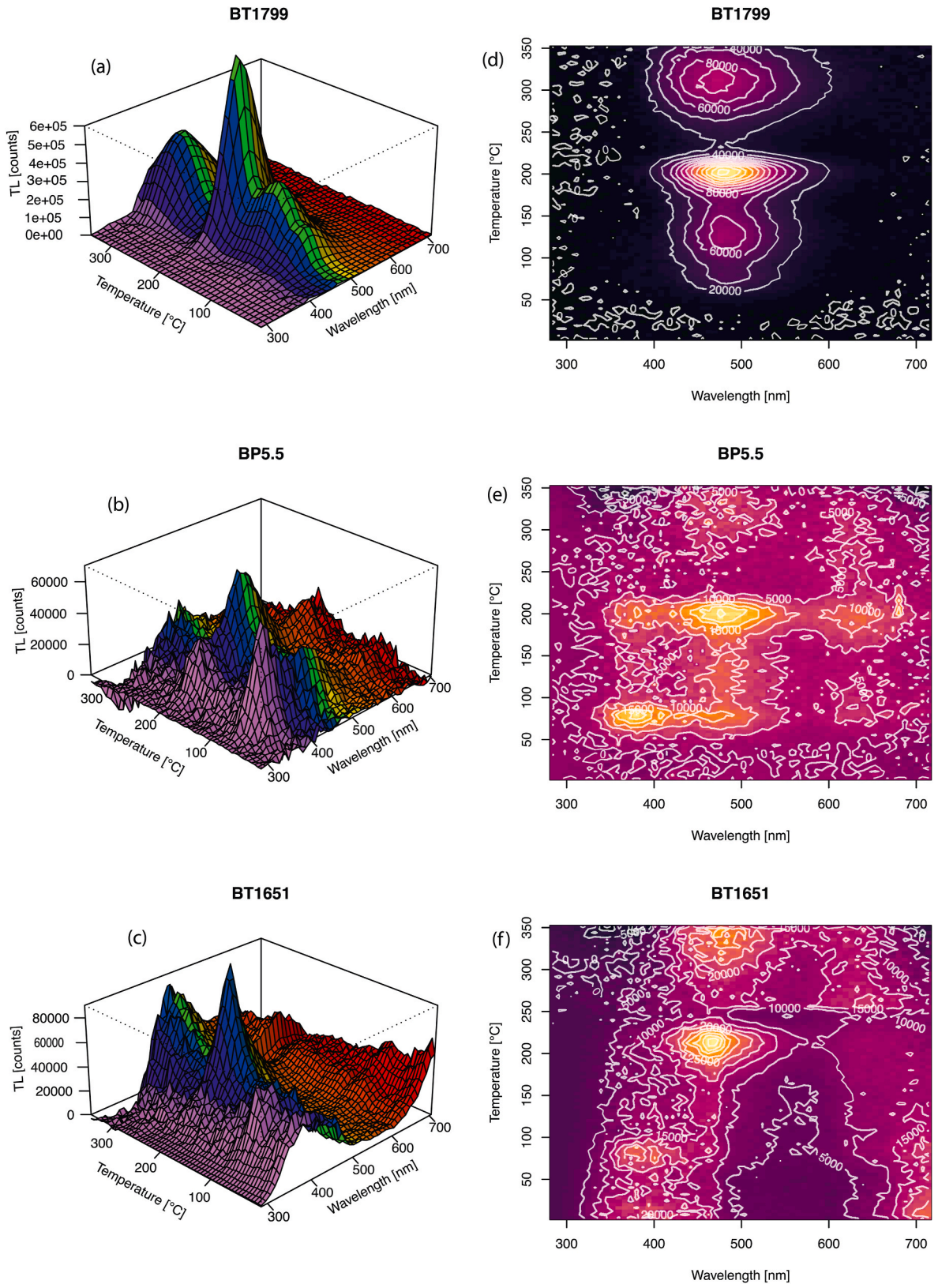

Fig. 2. Examples of 3D and 2D emission spectra of quartz samples BT1799 after a laboratory dose of 1 kGy (a, d), BP5.5 after a laboratory dose of 1 kGy (b, e) and BT1651 after a laboratory dose of 8 kGy (c, f).

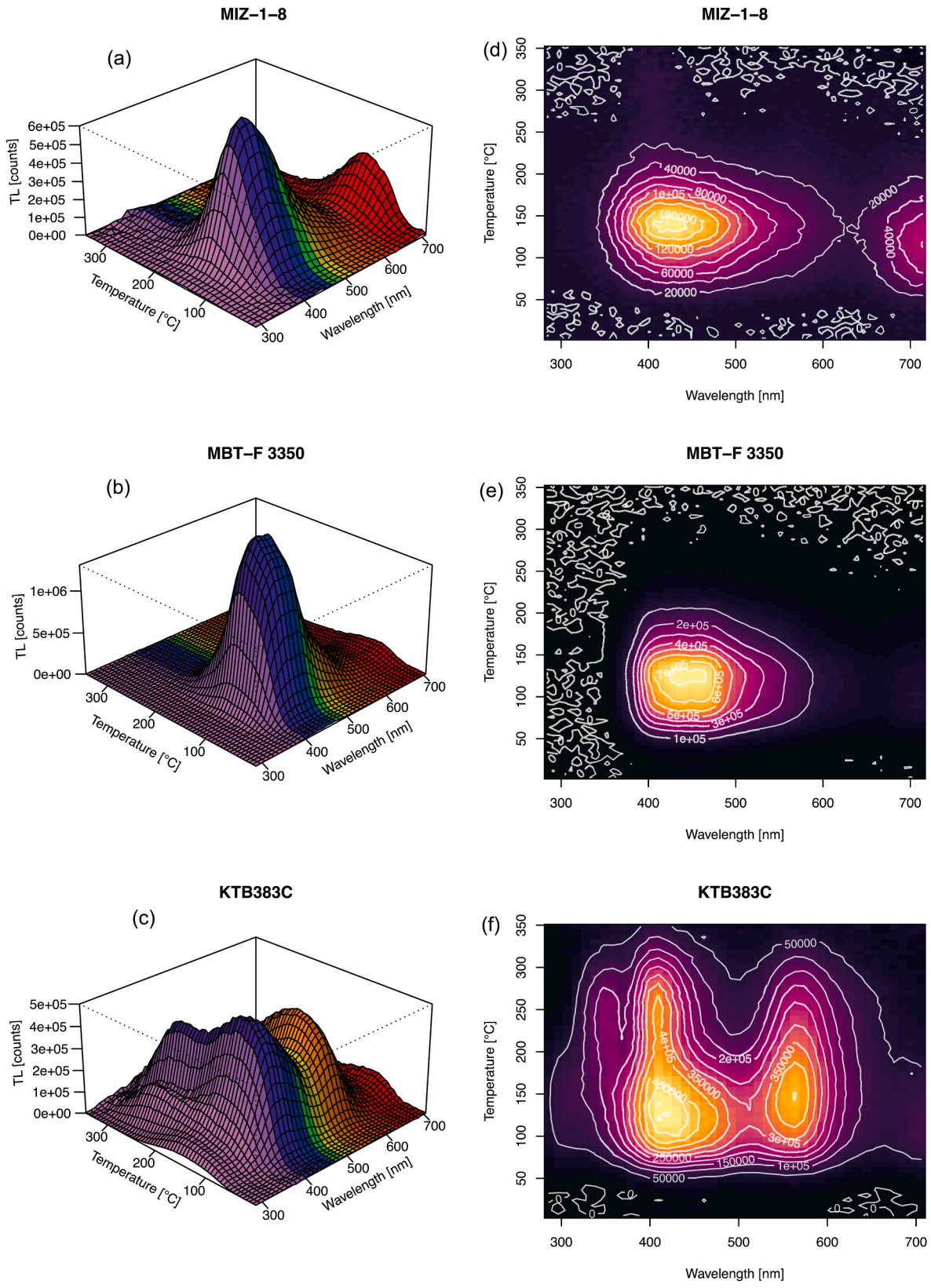

Fig. 3. Examples of 3D and 2D emission spectra of feldspar samples (a, d) MIZ-1-8, (b, e) MBT-F 3350, and (c, f) KTB383C, each following a dose of 500 Gy.

between these minerals. The most prominent distinctive feature for the spectrum of the Na-feldspar sample (KTB383C) is the additional intense emission band at ~580 nm that is well separated from the ~430 nm band.

3.3. Decomposition of emission spectra

The TL spectra of both irradiated quartz and feldspar samples were used to estimate the number and energy of emission bands in the

temperature region between 175 °C and 220 °C to study in detail the luminescence features of the 200 °C TL peak. The TL peaks in this temperature range are metastable and are sensitive to temperature fluctuations occurring at Earth's surface over geological timescales (Ronca and Zeller, 1965). Fig. 4 shows the Gaussian fits obtained for quartz and feldspar samples irradiated at various doses. It is evident that the blue emission band at ~2.5 eV (~480 nm) is present in all quartz samples in this study and dominant for BT1799 and BP5.5. It is the only emission that has been detected for sample BT1799 (Fig. 4a), while for sample BP5.5 a UV emission (at ~3.17 eV or ~319 nm) was detected in addition to the blue emission (Fig. 4b). The presence of two components of "blue" TL from a ground quartz crystal, one at 2.5 eV (480 nm) and another at 2.8 eV (440 nm), was reported by Martini et al. (2012). However, for our samples we only observed the 2.5 eV emission that dominates all quartz emission spectra for the 200 °C TL peak.

Unlike the other two quartz specimens, sample BT1651 shows an additional red emission (1.89 eV or ~660 nm). This red emission becomes clearer and is well defined at higher doses (>1 kGy) (Fig. 4c). The common feature of the spectra for quartz samples are firstly that the emission bands can be easily identified in terms for position (wavelength) and intensity, but they vary in number whereby samples from different provenances have different numbers of emission bands in the temperature intervals we investigated in this study. The three main emission bands of quartz are centred at about 360–420 nm (near UV to UV), 460–480 nm (blue) and 610–630 nm (orange-red) (Krbetschek et al., 1997; Lomax et al., 2015). In our samples, the blue emission is the most intense band for BT1799 and BP5.5, while red and UV emissions were also detected in BP5.5 and BT1651, respectively, and the emission peak locations are in accordance with those summarised in Krbetschek et al. (1997).

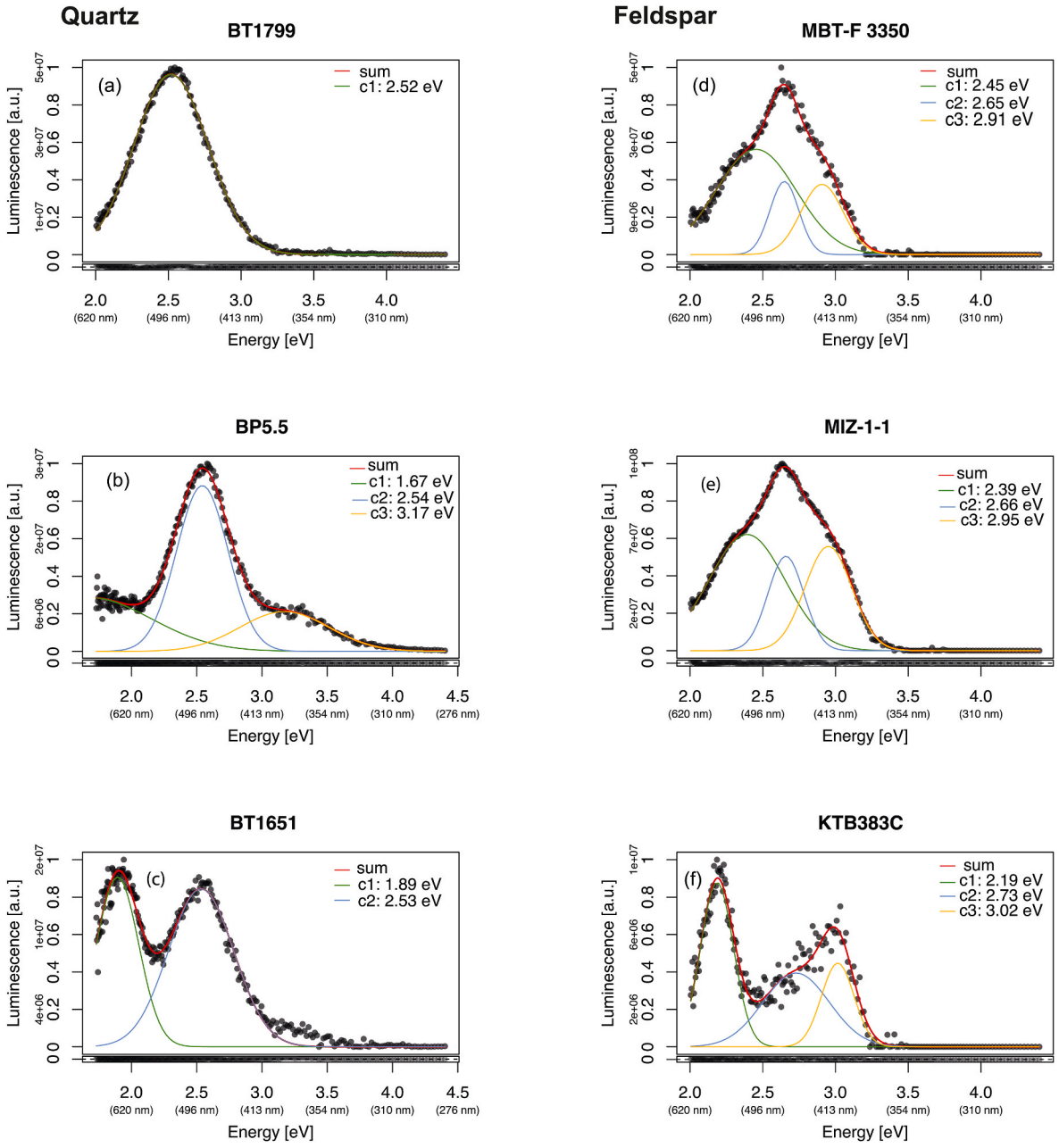

Fig. 4. Deconvolution into Gaussian components of the TL spectra of quartz samples (a) BT1799 after a laboratory dose of 4 kGy, (b) BT5.5 after a dose of 500 Gy, and (c) BT1651 after a dose of 4 kGy. For feldspar samples, the spectrum of (d) MBT-F 3350 was recorded after a dose of 500 Gy, those of (e) MIZ-1-1 and (f) KTB383C after a dose of 1 kGy each.

A series of previous investigations have attempted to relate the composition of quartz TL spectra to mineral forming process, provenance and/or sedimentary history, although universal conclusions are difficult to draw (e.g., Hashimoto et al., 1986; Hashimoto, 2008). However, it appears that the red TL emission (~1.90–1.95 eV or 630–650 nm) occurs more often for samples of volcanic origin, while the UV emission is rather associated with both plutonic and volcanic quartz. The samples studied here show all commonly reported TL emissions and their relative variations. The three samples are not considered representative of most other samples, but they provide an additional dataset on the variability in TL emission characteristics reported for quartz.

The TL spectra of feldspar in Fig. 4(d–f) have a common feature, which is the combination of at least three overlapping bands of relatively high intensity. They are located approximately at 2.4–2.5 eV, 2.6 eV and 2.9 eV for samples MBT-F3350 and MIZ-1-1 and at 2.2 eV, 2.7 eV and 3.0 eV for sample KTB383C. A difference was seen on the degree of overlap, whereby for the Na-feldspar (KTB383C), emission bands are more isolated (especially the one at 2.2 eV) compared to those of K-feldspars (MBT-F3550 and MIZ-1-1). We also observed the dominance of the blue emission for K-feldspar, while the yellow-green emission contributes almost equally for Na-feldspar.

For feldspar minerals, a variety of different TL emissions is reported (Fattahi and Stokes, 2003; Galean et al., 2006) and both quartz and feldspar emissions are reported to be composite. Whereas the quartz samples studied here exhibit emission bands comparatively well separated from each other in wavelength/energy space, TL bands for the feldspar samples show substantial overlap. Hence, broadband optical filters that are routinely used in luminescence applications would pass signals with different properties, representing a potential source of inaccuracy in luminescence thermometry and dosimetry. Knowledge on the emission wavelengths for samples under study is vital for choosing optimal filter combinations, enabling isolation of bands with desirable characteristics such as a specific thermal stability and high signal to noise ratio.

The four feldspar samples characterised in Table 1 display typical TL spectra of three emission bands following irradiation, with samples of the same chemistry producing spectra of the same structure and the same number of emission bands. Interested readers are referred to the study by Riedesel et al. (2021) that investigates the relationship between feldspar chemistry/structural state and TL emissions in more detail. As both K-feldspar and Na-feldspar displayed a strong UV-blue emission in the temperature range of our interest (175–220 °C), we selected the ~2.5–2.6 eV emission band of quartz (BT1799, BP5.5, BT1651) and K-feldspar (MBT-F 3350, MIZ-1-1), and the ~2.2 eV emission band for Na-feldspar (KTB383C) for the following dose response studies in the context of palaeothermometry.

3.4. Dose response

The effect of high-dose irradiation on the position and the sensitivity-corrected intensity of the blue emission band between 2.5 eV and 2.7 eV is shown in Figs. 5 and 6. The position of the emission band is the energy that corresponds to the maximum TL intensity of the fitted emission band at a specific dose. The position of the blue emission band is not affected by irradiation (Fig. 5). The first two data points (small doses) are shown to be at a higher energy position and have a comparably larger uncertainty than high dose points. This observation can potentially be attributed to the low TL signals and a consequently less robust fitting estimate of the energy position.

Since the decomposition of the 200 °C feldspar TL emission spectra in Fig. 4 indicated that the blue emission (~2.6−2.7 eV) is dominant, omnipresent and its TL maximum easy to record, the saturation behaviour of K-feldspar TL was investigated using this band. For KTB383C, the dose response (i.e., sensitivity corrected TL intensity) for the yellow-green (2.2 eV) emission is plotted in Fig. 6, along with a representative K-feldspar DRC (sample MTB-F 3350). For sample KTB383C, the blue emission (2.7 eV) (Fig. 4f), overlaps with two other emissions, and we cannot easily estimate the maximum TL intensity following irradiation, and for this specific sample, the dose response curve of the 2.2 eV (yellow-green) emission was investigated. Since we did not note any spectral changes following doses of 20 kGy and higher for our studied feldspar samples, we stopped dose response experiments at 20 kGy for sample KTB383C to save machine time.

Generally, the emission bands observed grow at different rates in response to the irradiation dose. For the studied quartz samples, the main effect of irradiation is the increase of the TL intensity of the blue emission band up to ~15 kGy for the sensitivity corrected signal (Fig. 6). For larger doses (>15 kGy), the signal exhibits dose quenching until 50 kGy. For the uncorrected signal, dose quenching starts after ~6 kGy (Fig. S1).

The behaviour of the dose response for quartz can be described as a relation between radiation-induced destruction and filling of the traps

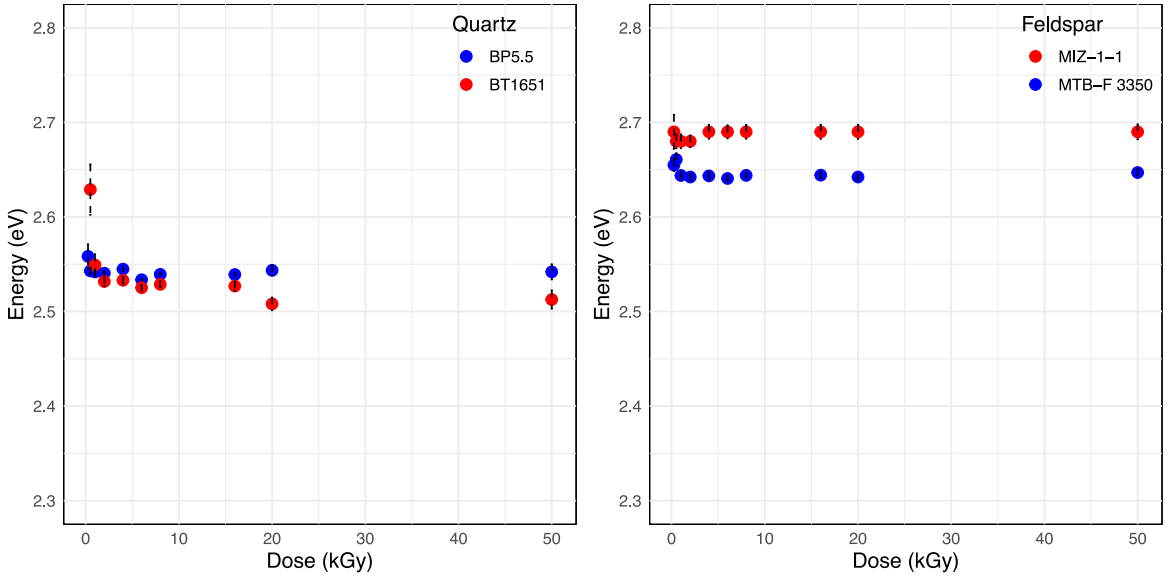

Fig. 5. Effect of irradiation dose on the position of the blue emission band for both quartz and feldspar.

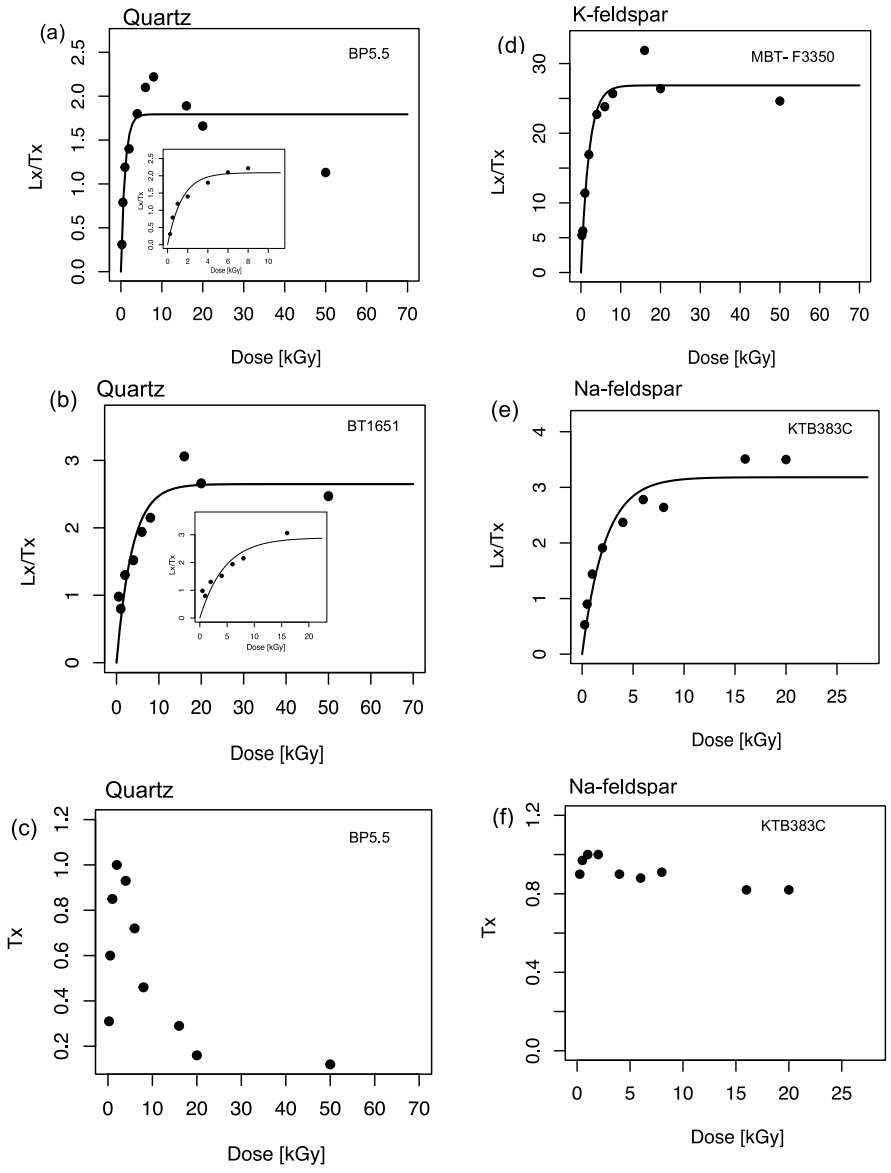

Fig. 6. Dose response of the sensitivity-corrected TL signal (L_x/T_x) for the blue (2.5 eV) emission band (a, b), and its test dose (T_x) response (c) for quartz, K-feldspar (d) exposed to beta-doses in the range 250 Gy–50 kGy, the yellow-green (2.2 eV) emission band for Na-feldspar (e) for doses up to 20 kGy and its test dose response (T_x) (f). The heating rate used is 1 °C s^{-1}. Dose response curves for feldspar samples were fitted with a single saturating exponential function. Insets in (a) and (b) are the fits of the increasing part of the dose response curves with a saturating exponential function.

(Sawakuchi and Okuno, 2004). For small doses, the number of empty traps is bigger than that of trapped charge carriers and the TL intensity increases with dose. Increasing dose, more traps are destroyed, and the remaining ones are all filled and therefore saturation is achieved. After saturation, more and more traps are destroyed and the TL intensity of the peak decays. The phenomenon of destruction of traps after high irradiation dose was also confirmed by the response of the TL intensity to the test dose normalised to the high intensity (Fig. 6c), where we observed the decrease in test dose TL intensity with prior regeneration dose. An alternative explanation might be double electron capture at trapping sites, analogous to the mechanism proposed by Woda and Wagner (2007) for the non-monotonic dose response of Ge- and Ti-centres in quartz.

For doses less than 6 kGy and the blue emission band (2.6 eV), the TL dose response is similar for the K-feldspar samples, i.e., the TL intensity increases monotonically. Administering higher doses (>6 kGy) does not result in substantial signal growth and the TL intensity stabilises after 10 kGy. The 2.2 eV emission for Na-feldspar (sample KTB383C) has the same dose response behaviour (Fig. 6). These observations suggest that saturation in TL response is reached above 6 kGy, with all electron traps with ambient temperature lifetimes longer than the irradiation time being filled. Most feldspar dose response curves were best fitted by a single saturating exponential function, verifying that a stable saturation level is reached in the kGy dose range. The characteristic saturation dose (D_0) extracted from the exponential rise was found to be in the order of 1.6 kGy.

4. Conclusion

The present study confirms the composite structure of TL spectra of quartz and feldspar and that the number and nature of TL emission bands varies across samples, depending on geochemical composition and sample history. While the emission bands of the quartz samples studied here are reasonably separated from each other in the energy space to capture single emissions by use of an optical bandpass filter, this is not the case for feldspar samples. Here, broadband, or bandpass

optical filtration of TL signals that is routinely used in luminescence applications would pass signals with different properties, coming from two or more individual TL emission bands with potentially different kinetic parameters. Thus, this spectral overlap is identified as a potential source of inaccuracy in luminescence palaeothermometry but also in luminescence dosimetry and dating (cf. Rink et al., 1993; Schmidt and Woda, 2019). Knowledge on the composition (number, maximum of emission energies but also full width at half maximum) of TL emission spectra for samples under study is therefore vital for choosing optimal filter combinations, enabling the isolation of bands with desirable characteristics such as appropriate thermal stability, saturation dose level and signal-to-noise ratio. Before starting the analyses of kinetic parameters of a (set of) sample(s) using monochromatic signals recorded with a PMT, we recommend first the screening of TL spectra following irradiation with a low and a high dose (close to saturation) to trace potentially interfering TL bands.

From the viewpoint of dose response, the quartz and feldspar samples investigated here display different behaviour. For quartz, the TL response made clear that high dose irradiation in combination with heat treatment substantially affected the kinetic behaviour of the system, which resulted in a signal decrease for doses >6 kGy. This non-monotonic TL signal evolution with dose inhibits defining a clear saturation level of TL, rendering the blue (~480 nm) TL signal at ~200 °C glow curve temperature potentially unsuitable for palaeothermometry and thermochronometry using the current approach of relative trap saturation levels (cf. King et al., 2016c). On the other hand, our data shows that the TL signal of feldspar saturates at high doses (>6 kGy) and the dose response curve is best fitted with a single saturating exponential function which renders feldspar minerals suitable for TL palaeothermometry and thermochronometry applications, as the relative trap saturation ratio is one of the key parameters required for temperature reconstruction.

CRediT authorship contribution statement

Pontien Niyonzima: Writing – original draft, Visualization, Methodology, Investigation, Formal analysis, Data curation. **Salome Oehler:** Writing – review & editing, Validation, Software, Investigation. **Georgina E. King:** Writing – review & editing, Validation, Supervision, Project administration, Funding acquisition. **Christoph Schmidt:** Writing – review & editing, Validation, Supervision, Software, Project administration, Methodology, Funding acquisition, Conceptualization.

Declaration of competing interest

The authors declare that they have no known competing financial interests or personal relationships that could have appeared to influence the work reported in this paper.

Data availability

The data are store in a repository that can be accessed via the following link: https://doi.org/10.48657/13ev-4995

Acknowledgements

This work was supported by the Swiss National Science Foundation (SNSF) under the grant number 200021_204236/1. We are grateful to Manabu Ogata and Shigeru Sueoka for providing samples from the Tono region in central Japan.

Appendix A. Supplementary data

Supplementary data to this article can be found online at https://doi.org/10.1016/j.radmeas.2024.107262.

References

Anechitei-Deacu, V., Timar-Gabor, A., Thomsen, K.J., Buylaert, J.P., Jain, M., Bailey, M., Murray, A.S., 2018. Single and multi-grain OSL investigations in the high dose range using coarse quartz. Radiat. Meas. 120, 124–130.

Autzen, M., Murray, A.S., Jain, M., Buylaert, J.P., 2021. Further investigations into the effect of charge imbalance on luminescence production. J. Lumin. 238, 118223.

Biswas, R.H., Herman, F., King, G.E., Braun, J., 2018. Thermoluminescence of feldspar as a multi-thermochronometer to constrain the temporal variation of rock exhumation in the recent past. Earth Planet Sci. Lett. 495, 56–68.

Biswas, R.H., Herman, F., King, G.E., Lehmann, B., Singhvi, A.K., 2020. Surface palaeothermometry using low temperature thermoluminescence of feldspar. Clim. Past 16, 2075–2093.

Bøtter-Jensen, L., Larsen, N.A., Mejdahl, V., Poolton, N., Morris, M., McKeever, S., 1995. Luminescence sensitivity changes in quartz as result of annealing. Radiat. Meas. 24, 535–541.

Brown, N.D., Rhodes, E.J., Harrison, T.M., 2017. Using thermoluminescence signals from feldspars for low temperature thermochronology. Quat. Geochronol. 42, 31–41.

Christodoulides, C., Ettinger, K.V., Fremlin, J.H., 1971. The use of TL glow peaks at equilibrium in the examination of the thermal and radiation history of materials. Mod. Geol. 2, 275–280.

Durrani, S., Prachyabrued, W., Christo-Doulides, C., Fremlin, J., Edgington, J., Chen, R., Blair, I., 1972. Thermoluminescence of Apollo 12 samples: implications for lunar temperature and radiation histories. In: Lunar and Planetary Science Conference Proceedings, p. 2955.

Durrani, S.A., Khazal, K.A.R., Ali, A., 1977. Temperature and duration of the shadow of a recently arrived lunar boulder. Nature 266, 411–415.

Fattahi, M., Stokes, S., 2003. Dating volcanic and related sediments by luminescence methods: a review. Earth Sci. Rev. 62, 229–264.

Fattahi, M., Stokes, S., 2000. Extending the time range of luminescence dating using red TL (RTL) from volcanic quartz. Radiat. Meas. 32, 479–485.

Gelian, G., Bin, X., Shunsheng, L., 2006. Study on feldspar thermoluminescence spectra and its luminescence dating implication. Nucl. Instrum. Methods Phys. Res. B 251, 143–147.

Gray, H.J., Jain, M., Sawakuchi, A.O., Mahan, S.A., Tucker, G.E., 2019. Luminescence as a sediment tracer and provenance tool. Rev. Geophys. 57, 987–1017.

Guimon, R., Weeks, K., Keck, B., Sears, D., 1984. Thermoluminescence as a palaeothermometer. Nature 311, 363–365.

Guralnik, B., Jain, M., Herman, F., Ankjærgaard, C., Murray, A.S., Valla, P.G., Preusser, F., King, G.E., Chen, R., Lowick, S.E., Kook, M., Rhodes, E.J., 2015. OSL thermochronology, of feldspar from the KTB borehole. Germany. Earth Planetary Science Letter 423, 232–243.

Hashimoto, T., 2008. An overview of red-thermoluminescence (RTL) studies on heated quartz and RTL application to dosimetry and dating. Geochronometria 30, 9–16.

Hashimoto, T., Koyanagi, A., Yokosaka, K., Hayashi, Y., Sotobayashi, T., 1986. Thermoluminescence color images from quartzs of beach sands. Geochem. J. 20, 111–118.

Herman, F., King, G.E., 2018. Luminescence thermochronometry: investigating the link between mountain erosion, tectonics, and climate. Elements 14, 33–38.

Herman, F., Rhodes, E.J., Braun, J., Heiniger, L., 2010. Uniform erosion rates and relief amplitude during glacial cycles in the Southern Alps of New Zealand, as revealed from OSL-thermochronology. Earth Planet Sci. Lett. 297, 183–189.

Hunter, P.G., Spooner, N.A., Smith, B.W., 2018. Thermoluminescence emission from quartz at 480 nm as a high-radiation marker. Radiat. Meas. 120, 143–147.

Huntley, D.J., Lamothe, M., 2001. Ubiquity of anomalous fading in K-feldspars and the measurement and correction for it in optical dating. Can. J. Earth Sci. 38, 1093–1106.

Kars, R.H., Wallinga, J., Cohen, K.M., 2008. A new approach towards anomalous fading correction for feldspar IRSL dating — tests on samples in field saturation. Radiat. Meas. 43, 786–790.

King, G.E., Guralnik, B., Valla, P.G., Herman, F., 2016c. Trapped charge thermochronometry and thermometry: a status review. Chem. Geol. 446, 3–17.

King, G.E., Herman, F., Guralnik, B., 2016b. Northward migration of the eastern Himalayan syntaxis revealed by OSL thermochronometry. Science 353 (6301), 800–804.

King, G.E., Herman, F., Lambert, R., Valla, P.G., Guralnik, B., 2016a. Multi-OSL thermochronometry of feldspar. Quat. Geochronol. 33, 76–87.

King, G.E., Tsukamoto, S., Herman, F., Biswas, R.H., Sueoka, S., Tagami, T., 2020. Electron spin resonance (ESR) thermochronometry of the Hida range of the Japanese Alps: validation and future potential. Geochronology 2, 1–15.

Kirsh, Y., Shova, L.S., Townsend, P.D., 1987. Kinetics and emission spectra of thermoluminescence in the feldspar albite and microcline. Phys.. stat. sol.(a) 101, 253.

Krbetschek, M.R., Götze, J., Dietrich, A., Trautmann, T., 1997. Spectral information from minerals relevant for luminescence dating. Radiat. Meas. 27, 695–748.

Kreutzer, S., 2023a. plot_RLum.Data.Spectrum( ): plot function for an RLum.Data. Spectrum S4 class object. Function version 0.6.8. In: Kreutzer, S., Burow, C., Dietze, M., Fuchs, M.C., Schmidt, C., Fischer, M., Friedrich, J., Mercier, N., Philippe, A., Riedesel, S., Autzen, M., Mittelstrass, D., Gray, H.J., Galharret, J. (Eds.), Luminescence : Comprehensive Luminescence Dating Data Analysis, 2023, R package version 0.9.22. https://CRAN.R-project.org/package=Luminescence.

Kreutzer, S., 2023b. fit_EmissionSpectra( ): luminescence emission spectra deconvolution. Function version 0.1.1. In: Kreutzer, S., Burow, C., Dietze, M., Fuchs, M.C., Schmidt, C., Fischer, M., Friedrich, J., Mercier, N., Philippe, A., Riedesel, S., Autzen, M., Mittelstrass, D., Gray, H.J., Galharret, J. (Eds.),

Luminescence : Comprehensive Luminescence Dating Data Analysis, 2023, R package version 0.9.22. https://CRAN.R-project.org/package=Luminescence.
Kreutzer, S., Schmidt, C., Fuchs, M.C., Dietze, M., Fischer, M., Fuchs, M., 2012. Introducing an R package for luminescence dating analysis. Ancient TL 30, 1–8.
Kuhn, R., Trautmann, T., Singhvi, A.K., Krbetschek, M.R., Wagner, G.A., Stolz, W., 2000. A study of thermoluminescence emission spectra and optical stimulation spectra of quartz from different provenances. Radiat. Meas. 32, 653–657.
Lambert, R., 2018. Investigating Thermal Decay in K-Feldspar for the Application of IRSL Thermochronometry on the Mont Blanc Massif. Unpublished PhD Thesis. University of Lausanne, Switzerland.
Lomax, J., Mittelstraß, D., Kreutzer, S., Fuchs, M., 2015. OSL, TL and IRSL emission spectra of sedimentary quartz and feldspar samples. Radiat. Meas. 81, 251–256.
Lowick, S.E., Preusser, F., Wintle, A.G., 2010. Investigating quartz optically stimulated luminescence dose–response curves at high doses. Radiat. Meas. 45, 975–984.
Martini, M., Fasoli, M., Villa, I., Guibert, P., 2012. Radioluminescence of synthetic and natural quartz. Radiat. Meas. 47, 846–850.
Murari, M.K., Kreutzer, S., King, G., Frouin, M., Tsukamoto, S., Schmidt, C., Lauer, T., Klasen, N., Richter, D., Friedrich, J., Mercier, N., Fuchs, M., 2021. Infrared radiofluorescence (IR-RF) dating: a review. Quat. Geochronol. 64, 101155.
Ogata, M., King, G.E., Herman, F., Sueoka, S., 2022. Reconstructing the thermal structure of shallow crust in the Tono region using multi-OSL-thermometry of K-feldspar from deep borehole core. Earth Planet Sci. Lett. 591, 117607.
Preusser, F., Chithambo, M.L., Götte, T., Martini, M., Ramseyer, K., Sendezera, E.J., Susino, G.J., Wintle, A.G., 2009. Quartz as a natural luminescence dosimeter. Earth Sci. Rev. 97, 184–214.
Preusser, F., Degering, D., Fuchs, M., Hilgers, A., Kadereit, A., Klasen, N., Krbetschek, M., Richter, D., Spencer, J.Q., 2008. Luminescence dating: basics, methods, and applications. E&G Quaternary Science Journal 57, 95–149.
Rahimzadeh, N., Tsukamoto, S., Zhang, J., Long, H., 2021. Natural and laboratory curves of quartz violet stimulated luminescence (VSL): exploring the multiple aliquot regenerative (MAR) protocol. Quat. Geochronol. 65, 101194.
Riedesel, S., Bell, A.M.T., Duller, G.A.T., Finch, A.A., Jain, M., King, G.E., Pearce, N.J., Roberts, H.M., 2021. Exploring sources of variation in thermoluminescence emissions and anomalous fading in alkali feldspars. Radiat. Meas. 141, 106541.
Rink, W., Rendell, H., Marseglia, E., Luff, B., Townsend, P., 1993. Thermoluminescence spectra of igneous quartz and hydrothermal vein quartz. Phys. Chem. Miner. 20, 353–361.
Ronca, L.B., Zeller, E.J., 1965. Thermoluminescence as a function of climate and temperature. Am. J. Sci. 263, 416–428.
Sawakuchi, G., Okuno, E., 2004. Effects of high gamma ray doses in quartz. Nucl. Instrum. Methods Phys. Res. B 218, 217–221.
Schilles, T., Poolton, N., Bulur, E., Bøtter-Jensen, L., Murray, A., Smith, G., Riedi, P., Wagner, G., 2001. A multi-spectroscopic study of luminescence sensitivity changes in natural quartz induced by high-temperature annealing. Journal of Physics D: Appl. Phys. 34, 722.
Schmidt, C., Woda, C., 2019. Quartz thermoluminescence spectra in the high-dose range. Phys. Chem. Miner. 46, 861–875.
Scholefield, R.B., Prescott, J.R., 1999. The red thermoluminescence of quartz: 3-D spectral Measurements. Radiat. Meas. 30, 83–95.
Stalder, N.F., Biswas, R.H., Herman, F., 2022. Maximized erosion at the last glacial maximum revealed by thermoluminescence. Quat. Geochronol. 73, 101405.
Tang, S.-L., Li, S.-H., 2015. Low temperature thermochronology using thermoluminescence signals from quartz. Radiat. Meas. 81, 92–97.
Thomsen, K.J., Murray, A.S., Jain, M., Bøtter-Jensen, L., 2008. Laboratory fading rates of various luminescence signals from feldspar-rich sediment extracts. Radiat. Meas. 43, 1474–1486.
Vainer, S., Schmidt, C., Garzanti, E., Ben Dor, Y., Pastore, G., Mokatse, T., Prud'homme, C., Leanni, L., King, G., ASTER Team, Verrecchia, E.P., accepted for publication. Chronology of sedimentation and landscape evolution in the Okavango Rift Zone, a developing young rift in southern Africa. J. Geophys. Res. Earth Surf.
Visocekas, R., Guérin, G., 2006. TL dating of feldspars using their far-red emission to deal with anomalous fading. Radiat. Meas. 41, 942–947.
Wintle, A.G., 1973. Anomalous fading of thermo-luminescence in mineral samples. Nature 245, 143–144.
Woda, C., Schilles, T., Riser, U., Mangini, A., Wagner, G.A., 2002. Point defects and the blue emission in fired quartz at high doses: a comparative luminescence and EPR study. Radiat. Protect. Dosim. 100, 261–264.
Woda, C., Wagner, G.A., 2007. Non-monotonic dose dependence of the Ge- and Ti-centres in quartz. Radiat. Meas. 42, 1441–1452.
Zhang, J., Li, S.H., 2020. Review of the post-IR IRSL dating protocols of K-feldspar. Methods and Protocols 3, 7.